



# 213 nm laser written waveguides in Ge-doped planar silica without hydrogen loading

PAUL C. GOW,<sup>\*</sup>  Q. SALMAN AHMED, PAOLO L. MENNEA, REX H. S. BANNERMAN,  ALEXANDER JANTZEN,  CHRISTOPHER HOLMES,  JAMES C. GATES,  CORIN B. E. GAWITH, AND PETER G. R. SMITH

*Optoelectronics Research Centre, University of Southampton, Southampton, SO17 1BJ, UK*

*\*p.gow@soton.ac.uk*

**Abstract:** In this paper we present the first example of waveguides fabricated by UV writing in non-hydrogen loaded Ge-doped planar silica with 213 nm light. Single mode waveguides were fabricated and the numerical apertures and mode field diameters were measured for a range of writing fluences. A peak index change of  $5.3 \times 10^{-3}$  was inferred for the waveguide written with  $70 \text{ kJ cm}^{-2}$ . The refractive index change is sufficient to match the index structure of standard optical fiber. Uniformity of the written structures was measured and a propagation loss of  $0.39 \pm 0.03 \text{ dB cm}^{-1}$  was determined through cutback measurements.

Published by The Optical Society under the terms of the [Creative Commons Attribution 4.0 License](https://creativecommons.org/licenses/by/4.0/). Further distribution of this work must maintain attribution to the author(s) and the published article's title, journal citation, and DOI.

## 1. Introduction

Integrated optical waveguides and circuits have a wide range of applications, including; sensing [1–4], and quantum technologies [5–7] to name but a few. These optical devices can be fabricated on a myriad of material platforms, each of which have their own advantages and drawbacks [8]. For instance, III-V semiconductors and silicon-based devices benefit from an established route for manufacture as well as high refractive indexes, allowing for compact optical circuits. However, additional losses are incurred during fibre coupling due to mode mismatch. Propagation losses can also be significant compared to other materials [8,9]. Silica-based optics offer low loss in the C-band as well as mode matching for optical fibre coupling. Etched silica devices are used for fibre compatible AWGs, sensors, and also quantum experiments [10]. However, propagation losses in etched waveguides are also strongly influenced by sidewall roughness and slope caused during the etching process [11,12].

Photonic structures can be created in planar doped silica without the need for etching by inducing a local refractive index change through exposure to a focused UV laser beam, as shown in Fig. 1(a). This technique has been used for phase tuning of optical devices [13] and to produce planar integrated circuits [14–17]. Losses are typically  $<0.2 \text{ dB/cm}$  [18] and waveguide modes are matched to optical fibres for optimum coupling efficiency. UV fabrication of integrated silica photonics relies on the photosensitivity provided by doping with Germanium, Phosphorous and Boron. However, it is usually necessary for in-diffusion of hydrogen or deuterium prior to UV writing to produce a refractive index change sufficient to form waveguides [19]. This is typically achieved by leaving the sample in a pressurised hydrogen environment for several days to allow diffusion in to the material [20].

Hydrogen loading not only requires further processing but, after removal from the pressurised environment, the hydrogen present within the silica out diffuses, causing photosensitivity variation over time. Hydrogen can also be depleted through writing adjacent features in close proximity, something necessary when writing devices such as beam splitters [21,22]. These effects can

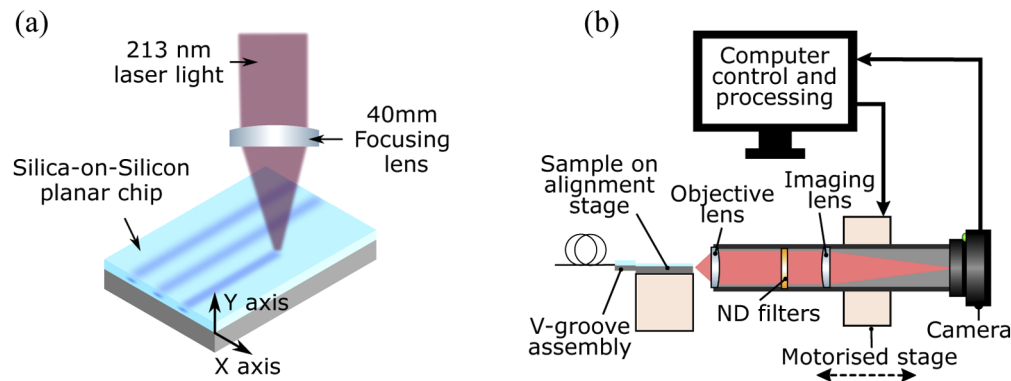


**Fig. 1.** (a) A set of precision air-bearing stages translate a planar silica-on-silicon chip through the focus of a 213 nm laser beam to write waveguides into the Ge-doped silica core layer. (b) Schematic of the characterisation system. Broadband light from an erbium-doped fiber ASE source is coupled into the waveguides via a fiber V-groove assembly and the waveguide facets are imaged directly onto an InGaAs camera interfaced with computer software.

cause variation of the final written structures and these issues scale with device complexity, something undesirable in applications such as quantum technology and sensing, which require device consistency and compact, integrated solutions [6,23].

It is possible to slow the rate of outgassing by cooling the substrate during writing [21], though this requires a cooled stage and nitrogen flow to prevent condensation forming, yet this does not prevent outgassing entirely. Another approach is to lock the hydrogen within the silica through UV exposure or thermal processing, allowing the sample to maintain photosensitivity throughout the writing process [24]. However, this is an additional process which can prove inconsistent between batches, and can introduce additional losses through increased OH absorption within the material [25]. Other methods, adopted for quantum applications, include writing many smaller modular devices that can be configured together later on [26].

Femtosecond laser writing is capable of producing photonic devices in planar and bulk silica without the need for hydrogen loading, with waveguide propagation losses as low as  $0.35 \text{ dB cm}^{-1}$  in the telecommunications C-band [27],  $0.2 \text{ dB cm}^{-1}$  for 633 nm [28], and refractive index changes of around  $10^{-3}$  [29]. A refractive index change of  $3 \times 10^{-3}$  in hydrogen-free Ge-doped planar silica layers using a 193 nm UV laser has been reported, however propagation losses were close to  $2.8 \text{ dB cm}^{-1}$  [30].

The work in this paper was inspired by the achievement of strong fiber Bragg gratings (FBGs) in Ge-doped optical fiber without prior hydrogen loading by using a nanosecond pulsed UV laser operating at 213 nm [31]. These gratings were produced through the phase mask technique and were shown to generate a higher photosensitivity than 248 nm light. To date, a maximum grating index modulation of  $1.1 \times 10^{-3}$  and overall index change of  $1.2 \times 10^{-3}$  has been achieved in B/Ge doped optical fibre without hydrogen loading. Index changes of this magnitude are required for planar silica, in which single-mode waveguides must be defined along with the gratings.

Here we present the first waveguides fabricated in Ge-doped planar silica through the direct UV writing (DUW) technique without hydrogen loading using a 213 nm UV laser. We characterise the numerical aperture and mode field diameter of each waveguide, as well as waveguide uniformity and loss. Writing without hydrogen loading and using the powers available with 213 nm light would allow paralleled writing of entire wafers, providing improved device performance and reduced costs in scaling up the DUW process.

## 2. Experimental method and results

In this section the characterisation of waveguides written with 213 nm UV light is discussed. The numerical aperture (NA) and mode field diameter (MFD) of each waveguide written with different fluences are compared and the resulting index change induced by the UV light is inferred. The uniformity of the written waveguides is measured and the propagation losses are determined through cutback measurements.

### 2.1. Experimental background

Similar doped silica-on-silicon samples to those reported in [32] were used in this study. These were fabricated through flame hydrolysis deposition (FHD). A 1 mm thick silicon wafer with a 15.0  $\mu\text{m}$  thermal oxide was used as a substrate and optical underclad. A 5.7  $\mu\text{m}$  silica layer doped with Germanium and Boron was deposited onto these chips by FHD to act as the core. The torch deposited a mixture of  $\text{SiCl}_4$  (135 sccm),  $\text{GeCl}_4$  (42 sccm), and  $\text{BCl}_3$  (61 l/min). This was then capped with a 7.3  $\mu\text{m}$  thick layer doped with  $\text{SiCl}_4$  (133 sccm),  $\text{PCl}_3$  (30 sccm), and  $\text{BCl}_3$  (69 l/min) to act as an overclad. Individual planar chips were diced from this wafer using a Loadpoint, MicroAce, Series 3 dicing machine. The source used for UV writing was a Xiton Photonics single frequency SLM-213 fifth-harmonic solid state laser operating at a wavelength of 213 nm and a 28 kHz repetition rate. The output beam was focused by a 40 mm focal length  $\text{CaF}_2$  lens to a  $1/e^2$  gaussian spot diameter of 3.75  $\mu\text{m}$  which was confirmed through knife edge measurements. Writing was performed at an average power of 5 mW, which equated to a peak pulse fluence of 11.4  $\text{J cm}^{-2}$  incident on the silica. This is close to the damage threshold of the glass, with low ablation rates previously shown at 20  $\text{J cm}^{-2}$  with a 193 nm source [33]. However, this depends strongly on surface quality of the silica under illumination, where increased roughness and surface contamination results in a reduced UV laser damage threshold [34]. The planar chip was mounted on a set of Aerotech precision air bearing stages and translated through the focus of the beam to write waveguides into the photosensitive core layer (Fig. 1(a)).

### 2.2. Fluence characterisation of waveguides

For each waveguide the writing fluence was altered by manipulation of the stage translation speed, therefore varying the induced refractive index change. In one experiment a total of fifteen straight waveguides were UV written along a planar doped silica-on-silicon chip of 15 mm length. Writing fluences ranged from 5 to 75  $\text{kJ cm}^{-2}$ , which are an order of magnitude larger than for hydrogen loaded 213 nm written waveguides [32]. This resulted in stage translation speeds from 1.9 to 0.12  $\text{mm min}^{-1}$ , giving a total time of approximately 14 hours to write all fifteen waveguides. Writing was done with at least 470 pulses per micron, ensuring continuous waveguides. The written chip was then mounted in the NA measurement setup, shown in Fig. 1(b), for characterisation of the NA and MFD of each waveguide. Broadband light from an erbium-doped fiber ASE source was coupled into the waveguides via a fiber V-groove assembly. The waveguides were characterised through imaging the waveguide facets directly onto an InGaAs camera interfaced with computer software. The camera and imaging lens were translated away from the waveguide facet and the software measured the divergence of the beam. The data was fitted using a second moment technique based on the standard detailed in ISO11146:2000 [35], which allowed the extraction of the NA, MFD and  $M^2$  parameters of both axes. The orientation is indicated in Fig. 1(a), where the X axis is defined as being perpendicular to the waveguide direction in the plane of the photosensitive core layer, and the Y axis is perpendicular to the planar core layer. These parameters were measured four times and the mean and standard deviation calculated and plotted in Fig. 2. The chip was initially characterised soon after writing and then stored for 14 months at standard room temperature and pressure. The chip was then re-measured and found to

have no temporal degradation of the induced index change or waveguide performance. All the data presented here are from this secondary characterisation.

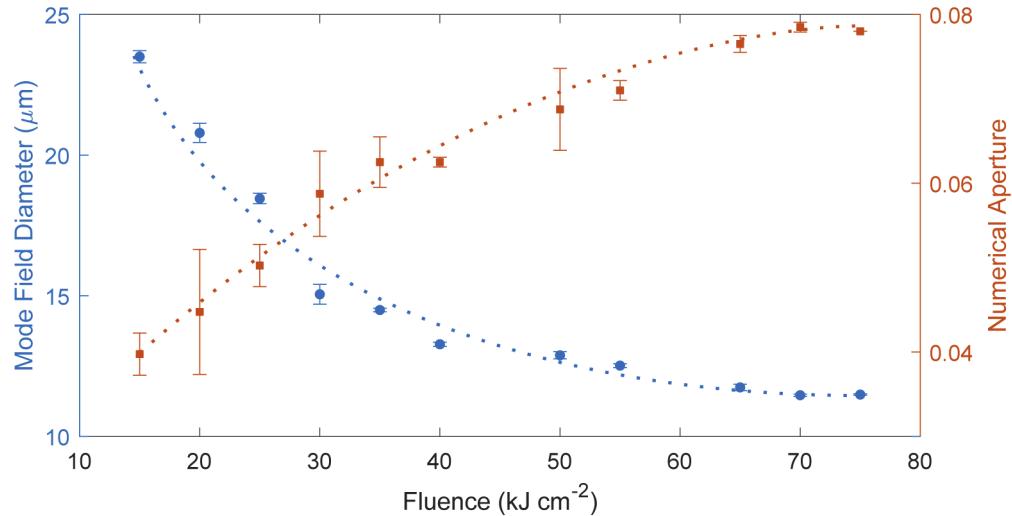


**Fig. 2.** The mode field diameter of the waveguides (blue circles, left) and the NA (orange squares, right) measured in the X axis are plotted against writing fluence. Dashed lines are provided to guide the eye. As the fluence increases the induced change in refractive index also increases, allowing the waveguide to better confine the mode. With increasing index contrast between the core and cladding layers the NA is shown to increase.

The results for the variation of MFD with writing fluence are plotted as blue circles in Fig. 2 (left axis). The standard deviations of the MFDs and NAs are represented as error bars on the plot. The MFD decreases with increasing fluence until achieving a minimum MFD of  $11.46 \pm 0.04 \mu\text{m}$  at the fluence of  $70 \text{ kJ cm}^{-2}$ . The refractive index change of the photosensitive silica is typically proportional to the fluence used to UV write [36], therefore higher fluence leads to stronger mode confinement in the waveguide. The average of the MFD's in the Y axis for all fluences was around  $10.71 \pm 0.24 \mu\text{m}$ . This is because the MFD in this axis is dictated by the thickness of the deposited photosensitive layer. To investigate coupling losses a PM1550 fibre V-groove assembly was measured in the NA setup to image its mode. An overlap integral was performed between this data and the modes of all of the waveguides to determine coupling efficiencies. This gave an estimate of losses due to coupling between the V-groove and the written waveguides. This analysis showed the lowest coupling loss achieved was  $0.773 \pm 0.001 \text{ dB}$  demonstrated by the waveguide written with  $70 \text{ kJ cm}^{-2}$ . This coupling efficiency could be improved by mode matching of the waveguides through control of the UV writing spot size and FHD layer thickness.

A continuous-wave frequency-doubled Argon-ion laser operating at 244 nm and an average power of 50 mW was used for comparison. 10 waveguides were written with fluences from 10 to  $100 \text{ kJ cm}^{-2}$  in a chip without hydrogen loading. In this case single mode waveguides were not achieved. Weak guiding was only evident in the waveguide written with a fluence of  $100 \text{ kJ cm}^{-2}$ , and demonstrated a large MFD of  $\sim 36 \mu\text{m}$ .

### 2.3. UV induced index change

The resulting NA measurements for the waveguides as a function of fluence are plotted as orange squares in Fig. 2 (right axis). The NA of a step-index waveguide can be used to estimate the induced refractive index change of the UV written waveguides. The FHD glass layers were individually measured on a Metricon prism coupler system to determine the refractive index of

the unwritten silica. This was determined to be  $1.4474 \pm 5 \times 10^{-5}$  for the core layer, measured with a laser wavelength of 1553 nm. Some guiding in the unwritten core was observed, suggesting a slightly raised refractive index in the core compared to the cladding layers. Layer indices are measured on separate test wafers, and therefore do not represent final layers where diffusion and thermal processes can change the index profile. This increase in index is most likely induced during furnace consolidation of the subsequent overclad layer through dopant diffusion. The unwritten core layer was initially modelled with a uniform refractive index to match the Y axis NA of the guiding observed. The model suggests a native increase of  $0.6 \times 10^{-3}$  of the core layer index compared to the cladding layers during consolidation.

To estimate the maximum index change achieved a waveguide was modelled using FIMMWAVE software. The underclad, core, and overclad layer thicknesses of 15.0, 5.7, and  $7.3 \mu\text{m}$  respectively were modelled. The maximum NA measured after UV writing indicates the waveguide with the largest peak refractive index change. The maximum mean NA measured in the X axis was  $0.079 \pm 0.001$  for a fluence of  $70 \text{ kJ cm}^{-2}$ . A gaussian index profile of  $3.75 \mu\text{m } 1/e^2$  width was used for the waveguide along the X direction to match that of the UV writing spot size, with the Y axis index modelled as uniform. This is based on the assumption that the index change is linear and not strongly saturating, resulting in a gaussian refractive index profile. Mode profiles for a range of refractive indices were modelled. The modelled mode profile for the  $70 \text{ kJ cm}^{-2}$  waveguide is shown in Fig. 3(a), with the measured diameters and actual image insets of the expanding beam shown in 3(b) for comparison. The maximum UV induced index change is measured as the peak value of the gaussian index profile, and was found to be  $5.3 \times 10^{-3}$ . This shows an index change high enough to yield an NA and mode-profile compatible with single mode 1550nm fibres. To our knowledge, this is the highest reported positive index change in germano-silicate glass without hydrogen loading.

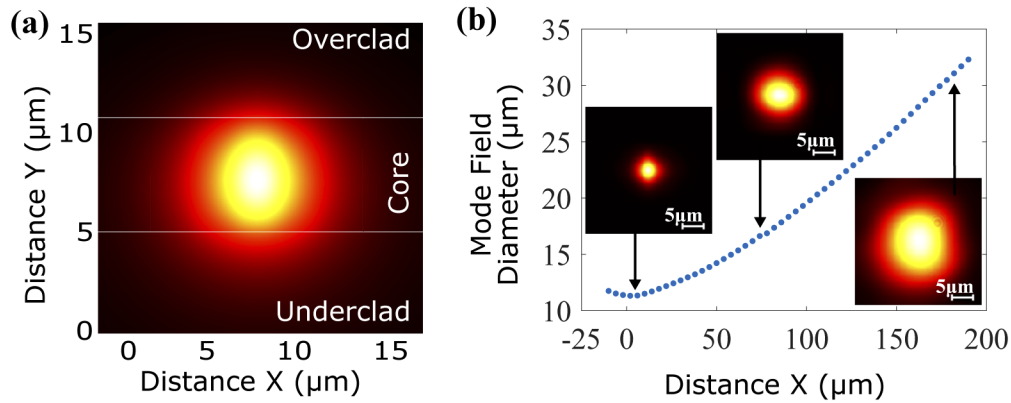


**Fig. 3.** (a) shows the FIMMWAVE model solution for the waveguide written with a fluence of  $70 \text{ kJ cm}^{-2}$ . This shows the intensity of the mode profile and gives an estimate for the peak index change achieved to be  $5.3 \times 10^{-3}$ . (b) shows a plot of the beam diameter data taken for the  $70 \text{ kJ cm}^{-2}$  waveguide. The insets show the actual images of the evolution of the mode as it expands from the waveguide facet.

#### 2.4. Waveguide uniformity and loss

Due to the long writing times involved with fabricating waveguides in doped silica without hydrogen loading, it is important to clarify the stability of the system for providing consistent results. To investigate uniformity 9 waveguides were written in a 15 mm long chip with a fluence of  $50 \text{ kJ cm}^{-2}$ . Writing time was 78 minutes per waveguide, giving a total time of around 12 hours to write the complete chip. The NA and MFD of each of these waveguides was then



measured and the standard deviation calculated. For the X axis the MFD was  $12.2 \pm 0.8 \mu\text{m}$ , and the NA was  $0.055 \pm 0.004$ . For the Y axis the MFD was  $10.4 \pm 0.2 \mu\text{m}$ , and the NA was  $0.084 \pm 0.002$ . This shows a good uniformity in the written waveguides despite the long writing time, in which laser power, temperature, and mechanical fluctuations could cause variations.

To measure the propagation loss of 213 nm hydrogen free waveguides, a chip measuring 6 cm in length was written with a fluence of  $60 \text{ kJ cm}^{-2}$ . This was pigtailed to a fiber V-groove assembly with UV cured glue and aligned in the cutback measurement setup shown in Fig. 4(a). The chip was aligned against a glass coverslip with refractive index matched oil to ensure consistent alignment position between cutbacks. Transmitted light was collimated and passed through an iris to remove stray and scattered light. The light was directed onto a detector to determine transmitted power, and the chip was removed, cleaned, and remeasured three times to eliminate further alignment discrepancies. The chip was diced back sequentially in 1 cm increments using the Loadpoint dicing machine with the pigtail remaining glued and aligned throughout. The transmitted power was then measured as above after each dicing increment. The transmission data is plotted in Fig. 4(b) and provides a propagation loss of  $0.39 \pm 0.03 \text{ dB cm}^{-1}$ . These results are consistent, to within the error, with other work using a 9 cm chip that was hydrogen loaded prior to UV writing with a 213 nm laser and gave a propagation loss of  $0.42 \pm 0.07 \text{ dB cm}^{-1}$  [30]. The loss values are large compared to the  $0.235 \pm 0.006 \text{ dB/cm}$  achieved previously with 244 nm written waveguides measured using a Bragg grating technique [37]. This difference in loss may be due to the thinner cladding layer used in this work, and in future devices the layer thickness could be increased to reduce loss. These losses could also indicate damage caused by the pulsed nature of the laser during writing, due to our operating close to the damage threshold.

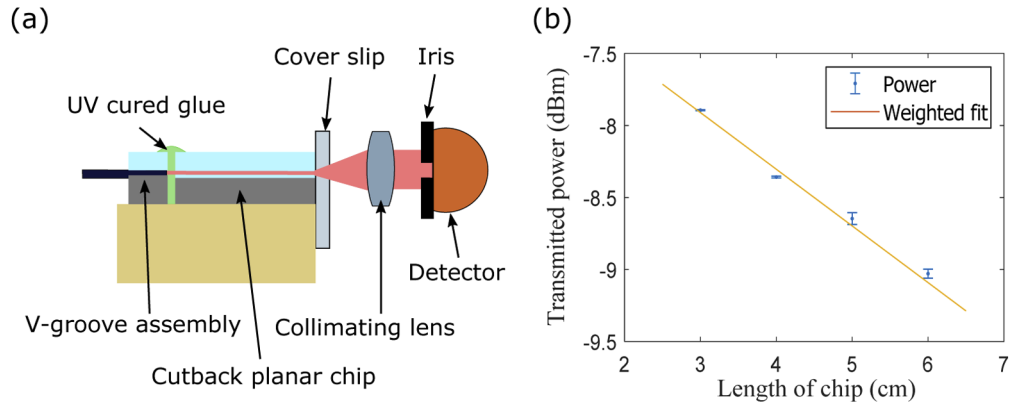


**Fig. 4.** (a) The characterisation setup for the cutback measurements is shown. The long waveguide chip is pigtailed and transmitted power is collimated and measured. The chip is aligned against a glass coverslip with refractive index matched oil to ensure consistent alignment position between cutbacks. (b) Transmitted power measured against chip length for cutback measurements performed on the 6 cm long chip written with  $60 \text{ kJ cm}^{-2}$ . The standard error of the measurements are plotted as error bars. The loss of  $0.39 \pm 0.03 \text{ dB cm}^{-1}$  is taken from the gradient and error in the gradient of the weighted fit.

### 3. Conclusion

Photonic waveguides were written in Ge-doped planar silica without hydrogen loading using a UV laser operating at 213 nm. The use of pulsed 213 nm UV light for small spot DUW allowed waveguides to be written without the need for hydrogen loading of the sample to increase photosensitivity. The NA of the waveguides was measured and gave a peak refractive index change

through modelling of  $5.3 \times 10^{-3}$  for a UV writing fluence of  $70 \text{ kJ cm}^{-2}$ . Cutback measurements were performed to find a propagation loss of  $0.39 \pm 0.03 \text{ dB cm}^{-1}$  in a hydrogen-free chip.

Inscription without hydrogen loading and the stability of the 213 nm laser provides a route to achieve greater uniformity for direct UV written integrated optics, generate precision diffractive structures, and UV write over large areas without variation due to out-diffusion of hydrogen. These features will be of notable use for quantum photonic applications and phase tuning of planar lightwave circuits. Future work will be to investigate the writing of Bragg gratings in planar silica with and without hydrogen using 213 nm light and investigation of waveguide losses in combination with laser pulse energies. We will also investigate increasing laser power and thus writing speed by using immersion or a thicker overlaid layer to reduce the power density at the surface.

(All data supporting this study are openly available from the University of Southampton repository at <https://doi.org/10.5258/SOTON/D1468>)

## Funding

Engineering and Physical Sciences Research Council (EP/M013243/1, EP/M013294/1, EP/M024539/1).

## Disclosures

The authors declare no conflicts of interest.

## References

1. C. Lavers, K. Itoh, S. Wu, M. Murabayashi, I. Mauchline, G. Stewart, and T. Stout, "Planar optical waveguides for sensing applications," *Sens. Actuators, B* **69**(1-2), 85–95 (2000).
2. P. V. Lambeck, "Integrated optical sensors for the chemical domain," *Meas. Sci. Technol.* **17**(8), R93–R116 (2006).
3. A. Jantzen, P. C. Gow, A. C. Gray, S. L. Scholl, J. C. Gates, P. G. R. Smith, L. J. Boyd, and C. Holmes, "Pressure sensing based on ratiometric Bragg grating loss in a planar silica diaphragm platform," in *Nonlinear Photonics*, (Optical Society of America, 2018), pp. JTu2A–62.
4. K. Schmitt, B. Schirmer, C. Hoffmann, A. Brandenburg, and P. Meyrueis, "Interferometric biosensor based on planar optical waveguide sensor chips for label-free detection of surface bound bioreactions," *Biosens. Bioelectron.* **22**(11), 2591–2597 (2007).
5. M. G. Thompson, A. Politi, J. C. Matthews, and J. L. O'Brien, "Integrated waveguide circuits for optical quantum computing," *IET Circuits, Devices & Systems* **5**(2), 94–102 (2011).
6. J. B. Spring, B. J. Metcalf, P. C. Humphreys, W. S. Kolthammer, X.-M. Jin, M. Barbieri, A. Datta, N. Thomas-Peter, N. K. Langford, D. Kundys, J. C. Gates, B. J. Smith, P. G. R. Smith, and I. A. Walmsley, "Boson sampling on a photonic chip," *Science* **339**(6121), 798–801 (2013).
7. J. P. Sprengers, A. Gaggero, D. Sahin, S. Jahanmirinejad, G. Frucci, F. Mattioli, R. Leoni, J. Beetz, M. Lermer, M. Kamp, and S. Höfling, "Waveguide superconducting single-photon detectors for integrated quantum photonic circuits," *Appl. Phys. Lett.* **99**(18), 181110 (2011).
8. S. Bogdanov, M. Shalaginov, A. Boltasseva, and V. M. Shalae, "Material platforms for integrated quantum photonics," *Opt. Mater. Express* **7**(1), 111–132 (2017).
9. F. Li, S. D. Jackson, C. Grillet, E. Magi, D. Hudson, S. J. Madden, Y. Moghe, C. O'Brien, A. Read, S. G. Duvall, and P. Atanackovic, "Low propagation loss silicon-on-sapphire waveguides for the mid-infrared," *Opt. Express* **19**(16), 15212–15220 (2011).
10. J. Carolan, C. Harrold, C. Sparrow, E. Martín-López, N. J. Russell, J. W. Silverstone, P. J. Shadbolt, N. Matsuda, M. Oguma, M. Itoh, G. D. Marshall, M. G. Thompson, J. C. F. Matthews, T. Hashimoto, J. L. O'Brien, and A. Laing, "Universal linear optics," *Science* **349**(6249), 711–716 (2015).
11. R. Deri, R. Hawkins, and E. Kapon, "Rib profile effects on scattering in semiconductor optical waveguides," *Appl. Phys. Lett.* **53**(16), 1483–1485 (1988).
12. K. P. Yap, A. Delâge, J. Lapointe, B. Lamontagne, J. H. Schmid, P. Waldron, B. A. Syrett, and S. Janz, "Correlation of scattering loss, sidewall roughness and waveguide width in silicon-on-insulator (SOI) ridge waveguides," *J. Lightwave Technol.* **27**(18), 3999–4008 (2009).
13. K. Takada and M. Abe, "UV trimming of AWG devices," in *Bragg Gratings, Photosensitivity, and Poling in Glass Waveguides*, (Optical Society of America, 2003), p. TuA1.
14. M. Svalgaard, C. V. Poulsen, A. Bjarklev, and O. Poulsen, "Direct UV writing of buried singlemode channel waveguides in Ge-doped silica films," *Electron. Lett.* **30**(17), 1401–1403 (1994).

15. M. Svalgaard, "Direct writing of planar waveguide power splitters and directional couplers using a focused ultraviolet laser beam," *Electron. Lett.* **33**(20), 1694–1695 (1997).
16. F. Knappe, J. Voigt, H. Renner, and E. Brinkmeyer, "Direct UV writing of multimode-interference couplers," in *Bragg Gratings, Photosensitivity, and Poling in Glass Waveguides*, (Optical Society of America, 2003) p.TuA4.
17. C. Sima, J. C. Gates, H. L. Rogers, P. L. Mennea, C. Holmes, M. N. Zervas, and P. G. R. Smith, "Ultra-wide detuning planar Bragg grating fabrication technique based on direct UV grating writing with electro-optic phase modulation," *Opt. Express* **21**(13), 15747–15754 (2013).
18. M. Svalgaard and M. Kristensen, "Directly UV written silica-on-silicon planar waveguides with low loss," *Electron. Lett.* **33**(10), 861–863 (1997).
19. M. Fokine and W. Margulis, "Large increase in photosensitivity through massive hydroxyl formation," *Opt. Lett.* **25**(5), 302–304 (2000).
20. P. J. Lemaire, R. M. Atkins, V. Mizrahi, and W. A. Reed, "High pressure H<sub>2</sub> loading as a technique for achieving ultrahigh UV photosensitivity and thermal sensitivity in GeO<sub>2</sub> doped optical fibres," *Electron. Lett.* **29**(13), 1191–1193 (1993).
21. K. Faerch and M. Svalgaard, "Symmetrical waveguide devices fabricated by direct UV writing," *IEEE Photonics Technol. Lett.* **14**(2), 173–175 (2002).
22. F. R. M. Adikan, "Direct UV-written waveguide devices," Ph.D. thesis, University of Southampton (2007).
23. C. Holmes, J. C. Gates, L. G. Carpenter, H. L. Rogers, R. M. Parker, P. A. Cooper, S. Chaotan, F. R. M. Adikan, C. B. E. Gawith, and P. G. R. Smith, "Direct UV-written planar Bragg grating sensors," *Meas. Sci. Technol.* **26**(11), 112001 (2015).
24. M. Åslund, J. Canning, and G. Yoffe, "Locking in photosensitivity within optical fiber and planar waveguides by ultraviolet preexposure," *Opt. Lett.* **24**(24), 1826–1828 (1999).
25. J. Stone, "Interactions of hydrogen and deuterium with silica optical fibers: A review," *J. Lightwave Technol.* **5**(5), 712–733 (1987).
26. P. L. Mennea, W. R. Clements, D. H. Smith, J. C. Gates, B. J. Metcalf, R. H. S. Bannerman, R. Burgwal, J. J. Renema, W. S. Kolthammer, I. A. Walmsley, and P. G. R. Smith, "Modular linear optical circuits," *Optica* **5**(9), 1087–1090 (2018).
27. Y. Nasu, M. Kohtoku, and Y. Hibino, "Low-loss waveguides written with a femtosecond laser for flexible interconnection in a planar light-wave circuit," *Opt. Lett.* **30**(7), 723–725 (2005).
28. H. Zhang, S. M. Eaton, and P. R. Herman, "Low-loss type ii waveguide writing in fused silica with single picosecond laser pulses," *Opt. Express* **14**(11), 4826–4834 (2006).
29. V. R. Bhardwaj, E. Simova, P. Corkum, D. Rayner, C. Hnatovsky, R. Taylor, B. Schreder, M. Kluge, and J. Zimmer, "Femtosecond laser-induced refractive index modification in multicomponent glasses," *J. Appl. Phys.* **97**(8), 083102 (2005).
30. J. Huebner, C. V. Poulsen, J. E. Pedersen, M. R. Poulsen, T. Feuchter, and M. Kristensen, "UV-written Y-splitter in Ge-doped silica," in *Functional Photonic and Fiber Devices*, vol. 2695 (International Society for Optics and Photonics, 1996), pp. 98–105.
31. M. Gagné and R. Kashyap, "New nanosecond Q-switched Nd:VO<sub>4</sub> laser fifth harmonic for fast hydrogen-free fiber Bragg gratings fabrication," *Opt. Commun.* **283**(24), 5028–5032 (2010).
32. P. C. Gow, R. H. S. Bannerman, P. L. Mennea, C. Holmes, J. C. Gates, and P. G. R. Smith, "Direct UV written integrated planar waveguides using a 213 nm laser," *Opt. Express* **27**(20), 29133–29138 (2019).
33. J. Ihlemann, B. Wolff, and P. Simon, "Nanosecond and femtosecond excimer laser ablation of fused silica," *Appl. Phys. A* **54**(4), 363–368 (1992).
34. J. Huang, F. Wang, H. Liu, F. Geng, X. Jiang, L. Sun, X. Ye, Q. Li, W. Wu, W. Zheng, and D. Sun, "Non-destructive evaluation of UV pulse laser-induced damage performance of fused silica optics," *Sci. Rep.* **7**(1), 16239 (2017).
35. ISO11146, "Lasers and laser-related equipment - Test methods for laser beam parameters - Beam width, divergence, angle and beam propagation factor," Standard, International Organization for Standardization, Geneva, CH (1999).
36. S. A. Slattery, D. N. Nikogosyan, and G. Brambilla, "Fiber Bragg grating inscription by high-intensity femtosecond UV laser light: comparison with other existing methods of fabrication," *J. Opt. Soc. Am. B* **22**(2), 354–361 (2005).
37. H. L. Rogers, S. Ambran, C. Holmes, P. G. R. Smith, and J. C. Gates, "In situ loss measurement of direct UV-written waveguides using integrated Bragg gratings," *Opt. Lett.* **35**(17), 2849–2851 (2010).